JMEPEG (2005) 14:565-568
DOI: 10.1361/105994905X64648

1059-9495/$19.00

# Experimental and Gas Phase Modeling of Nanocrystalline Diamond Films Grown on Titanium Alloys for Biomedical Applications

*M.J. Jackson, A.N. Jones, and W. Ahmed*

*(Submitted July 14, 2005; in revised form July 22, 2005)*

**For biomedical applications, it is highly desirable to be able to deposit smooth adherent diamond films on various complex-shaped substrates using the hot filament chemical vapor deposition technique (HFCVD). The properties of these films are affected profoundly by process parameters such as filament temperature, gas composition, and pressure. In this study, we present an insight into the gas phase chemistry involved in HFCVD of smooth nanocrystalline diamond films using $Ar/CH_4/H_2$ precursor mixtures. Experimental results on the growth, surface morphology, and crystalline structure are also presented. It is evident that the addition of a noble gas such as argon has a considerable effect on the gas surface chemistry. Notably at high concentrations of inert gas dilution (>90 vol.% argon) there are significant changes in diamond crystallinity ranging from polycrystalline through microcrystalline, and at argon concentrations >98 vol.%, nanocrystalline facets are observed. Modeling of the gas phase chemistry showed that the relative concentrations of $CH_3$ and $C_2H$ alter significantly in this region, and these in turn influence surface morphology and crystallinity of the deposited films.**

**Keywords** gas phase chemistry, HFCVD, modeling, nanocrystalline diamond

## 1. Introduction

Chemical vapor deposition (CVD) is a well-established process for the deposition of polycrystalline diamond films (Ref 1). However, for highly demanding applications such as biomedical components the diamond film surface is too rough. To decrease the crystal size and reduce the surface roughness, inert gases such as argon (Ar) and helium (H) can be added to the $CH_4/H_2$ precursor gases. The growth of nanocrystalline diamond films using CVD has recently attracted considerable attention because of its wide range of potential applications in biomaterials and micromechanical, microelectrical, optical, and electronic materials. Diamond coatings with a grain size in the order of 2-20 nm, known as nanocrystalline diamond (NCD), are well suited to these applications. Several approaches to the deposition of NCD films have been reported, including the use of fullerene precursors (Ref 2-5) and using $CH_4$ in $H_2$, or argon-rich plasmas at high pressures (Ref 6).

The influence of pressure on the nonequilibrium plasma chemistry of $C_2$, $C_2H$, $C_2H_2$, $CH_3$, $CH_4$, and H has been studied in plasma chemistry systems (Ref 7). To date little research has been conducted concerning the role of adding Ar to a hot filament CVD (HFCVD) system and modeling of the precursor gas phase species at low pressures and increased deposition temperatures. Extensive research into the nature of the precursor species for NCD films in microwave environments has been published (Ref 8-12) with considerable debate as to whether $C_1$ or $C_2$ growth precursors dominate the gas phase chemistry and are the major growth species for NCD deposition. Measurements of the carbon species concentration in hot filament or microwave systems using cavity ring-down spectroscopy (Ref 9, 13) have been carried out.

The kinetic modeling of the HFCVD has been investigated over a range of Ar concentrations suitable for NCD growth. The pressure and temperature of the system have been varied to examine the $CH_4$, $C_2H$, $C_2$, and $C_2H_2$ mole fractions at variable partial pressures and close to the filament temperature. We have modeled hot filament-assisted NCD growth in an Ar-rich environment (typically 0-99 vol.%) with the addition of molecular H (1-99 vol.%) and 1 vol.% $CH_4$.

## 2. Experimental Procedures

### 2.1 NCD Growth Experiments

NCD was deposited to titanium alloy substrates, using a HFCVD system described previously (Ref 14, 15). The precursor gas, $CH_4$ (1 vol.%) was diluted in Ar (0-99 vol.%) with additions of $H_2$ (0-99 vol.%). All films were deposited at a substrate temperature of 900 K, using a gas pressure of 2660 Pa throughout deposition. Prior to deposition, all substrates were negatively biased for 30 min, at −300 V (3 vol.% $CH_4$) to provide nucleation sites for subsequent diamond film growth (Ref 16). Diamond films were characterized in terms of crystal size and orientation using Raman spectroscopy (Kaiser Holoprobe) with a 532 nm Nd:YAG laser as the excitation source. X-ray diffraction spectra (XRD) generated from a Philips W170 diffractometer (Philips Instruments, San Diego, CA) were used for further confirmation of the film quality. The morphology of the NCD films was investigated using a Jeol

---

**M.J. Jackson,** Birck Nanotechnology Center, College of Technology, Purdue University, West Lafayette, IN 47907-2021; **A.N. Jones** and **W. Ahmed,** Dalton Research Institute, Manchester Metropolitan University, Manchester, M1 5GD, U.K. Contact e-mail: jacksomj@purdue.edu.

**Table 1 Reactions used in modeling calculations for NCD growth**

| Reaction | $A$ | $\beta$ | $E_a$, kcal mol$^{-1}$ | Ref |
|---|---|---|---|---|
| $H + H + M \rightarrow H_2 + M$ | 9.E + 16 | −0.6 | 0 | 18 |
| $H + H + M \rightarrow H_2 + M$ | 1.E + 18 | −1.0 | 0 | 19 |
| $H + CH_4 \rightarrow CH_3 + H_2$ | 6.6E + 08 | 1.6 | 10,840 | 20 |
| $CH_3 + H + M \rightarrow CH_4 + M$ | 8.0E + 26 | −3.0 | 0 | 21 |
| $CH_4 + CH_2 \rightarrow CH_3 + CH_3$ | 2.46E + 6 | 2.0 | 8,270 | 22 |
| $CH_4 + H = CH_3 + H_2$ | 6.60 | 1.6 | 10,840 | 23 |
| $CH_3 + CH_3 = C_2H_5 + H$ | 6.84E + 12 | 0.1 | 10,600 | 21 |
| $CH_3 + CH_3 + M = C_2H_6 + M$ | 3.18E + 41 | −7.0 | 2,766 | 20 |
| $CH_3 + H = CH_2 + H_2$ | 7.2E + 14 | 0.0 | 15,100 | 21 |
| $CH_3 + CH_2 = C_2H_4 + H$ | 4.0E + 13 | 0.0 | 0 | 19 |
| $CH_3 + M = CH_2 + H + M$ | 1.0E + 16 | 0.0 | 90,600 | 19 |
| $CH_2 + H = CH + H_2$ | 4.0E + 13 | 0.0 | 0 | 19 |
| $CH + CH_4 = C_2H_4 + H$ | 6.0E + 13 | 0.0 | 0 | 24 |
| $CH + CH_3 = C_2H_3 + H$ | 3.0E + 13 | 0.0 | 0.0 | 25 |
| $CH + H = C + H_2$ | 1.65E + 14 | 0.0 | 0.0 | 26 |
| $CH + CH_2 = C_2H_2 + H$ | 4.0E + 13 | 0.0 | 0.0 | 25 |
| $C + CH_3 = C_2H_2 + H$ | 5.0E + 13 | 0.0 | 0.0 | 25 |
| $C + CH_2 = C_2H + H$ | 5.0E + 13 | 0.0 | 0.0 | 25 |
| $C_2H_6 + H = C_2H_5 + H_2$ | 1.15e + 8 | 1.9 | 7,530 | 23 |
| $C_2H_6 + CH_3 = C_2H_5 + CH_4$ | 6.14E + 6 | 1.7 | 10,450 | 21 |
| $C_2H_6 + M = CH_3 + CH_3 + M$ | 1.0E + 19 | 0.0 | 68,000 | 20 |
| $CH_2 + CH_4 \rightarrow CH_3 + CH_3$ | 2.46E + 6 | 2.0 | 8,270 | 22 |
| $CH_3 + C_2H_4 \rightarrow C_2H_3 + CH_4$ | 2.27E + 5 | 2.0 | 9,200 | 21 |
| $CH + H_2 \rightarrow H + CH_2$ | 1.08E + 14 | 0.0 | 3,110 | 27 |
| $CH_2 + CH2 \rightarrow H + H + C_2H_2$ | 2.00E + 14 | 0.0 | 10,989 | 28 |

scanning electron microscope (SEM, model JSM 5600LV) and atomic force microscopy (AFM) using a silicon tip, performed in the contact mode with a force constant of 0.12 nm$^{-1}$ (Quesant Instruments, Agoura Hills, CA).

### 2.2 Computer Simulations

A CHEMKIN (Reaction Design, San Diego, CA) modeling package was used to perform the gas phase kinetic modeling, which uses the SENKIN modeling code (Ref 17). SENKIN is a simple one-dimensional kinetic model for studying nonequilibrium gas phase chemistry, which does not take into account all of the mass transport mechanisms. However, the model may be taken as a characteristic of the gaseous mole fractions close to the filament. The filament temperature was varied between 1400 and 2400 K. The system pressure remained constant at 2660 Pa. The elementary chemical reactions considered in the modeling calculations along with the corresponding kinetic data are shown in Table 1 (Ref 18-28). CHEMKIN merges gas phase reaction mechanisms into numerical simulations; it subsequently determines the mole fraction of differing species to predict homogeneous gas phase chemical kinetics. The rate of the forward reaction is calculated kinetically using a modified Arrhenius equation:

$$k = AT^{\beta} \exp^{\left(\frac{-E_a}{RT}\right)} \qquad \text{(Eq 1)}$$

where k is the rate constant, $E_a$ is the activation energy (J mol$^{-1}$), $A$ is the frequency factor (mol/cm$^3$ s$^{-1}$), R is the molar gas constant (8.3145 J K$^{-1}$ mol$^{-1}$), $T$ is the temperature (K), and $\beta$ is the temperature exponent. The following species were considered in the model: $C_2H$, $C_2H_6$, $C_2H_5$, $C_2H_4$, $C_2H_3$, $C_2H_2$, $CH_4$, $CH_3$, $CH_2$, CH, C, H, $H_2$, and Ar.

## 3. Results and Discussion

### 3.1 Diamond Growth

Figure 1(a) shows a diamond film deposited for 4 h, using 1 vol.% $CH_4$ in 99 vol.% $H_2$, without the presence of Ar. The films were nucleated in situ prior to deposition using a negative biased voltage of 300 V for 30 min. Negatively biasing the substrate causes the positively charged species in the plasma to bombard the surface of the substrate, thus creating nucleation sites for subsequent diamond growth. Examination of the films grown by HFCVD shows that the crystals are well-faceted and pyramidal shaped, the average crystallite size is ~2 μm, and the surface morphology is rough.

The addition of Ar to the gas mixture alters the plasma characteristics, and these are reflected in the as-grown films. When Ar is added there are notable changes in the crystallinity of the films with a significant decrease in the average crystallite size. Figure 1(b) shows a SEM image of a diamond film deposited on titanium alloy for 4 h using 1 vol.% $CH_4$ in 90 vol.% Ar/9 vol.% $H_2$ after 30 min of bias-enhanced nucleation (BEN). The films are microcrystalline, with facets typically oriented along the {111} crystal plane, where diamond crystals are approximately 400 nm. Figure 1(c) shows a SEM image of diamond deposited on titanium alloy for 4 h using 1 vol.% $CH_4$ in 98 vol.% Ar/1 vol.% $H_2$. There is a significant decrease in crystallinity; the film exhibits nanocrystalline type structures with a crystallite grain size of approximately 10 nm. The film thickness from the SEM analyses is observed to be approximately 100 nm. An AFM image of the diamond film deposited using 99 vol.% Ar/1% $CH_4$ is shown in Fig. 2, the area scanned is 5 by 5 μm. The films are uniform with a mean surface roughness ($R_a$) of 54.14 nm. The films are smooth with no apparent voids or pits across the surface.

### 3.2 SENKIN Modeling

Modeling investigations were performed at the temperature typically used for diamond growth, 2200 K with a pressure of 2660 Pa. The reaction time was sufficient for the species concentrations to reach equilibrium. Results show that with increasing argon concentration the $CH_3$ radical mole fraction decreases almost linearly (Fig. 3) The mole fraction of $C_2H_2$ (not shown) remains almost constant regardless of the initial Ar concentration, with a mole fraction value of $\sim 4.9 \times 10^{-3} \pm 0.1 \times 10^{-3}$. The model used here does not take into account reaction paths of the $C_2$ dimer, therefore $C_2H$ mole fractions were used to gauge the level of $C_2$ concentrations. Figure 3 shows that the $C_2H$ mole fraction remains approximately constant at Ar concentrations below ~85%. However, at higher Ar concentrations the mole fraction of $C_2H$ species increases rapidly and becomes the dominant growth species. Interestingly, in the as-grown diamond films there is a profound change in the crystal structure with the addition of high proportions of Ar to the input gas mixture, as seen from the SEM in Fig. 1. Without Ar, the growth rate is approximately 2 μm h$^{-1}$. However, when Ar is added, the growth rate initially increases to approximately 6 μm h$^{-1}$ and then decreases at high Ar concentrations to about 0.05 μm h$^{-1}$ at >90 vol.% Ar. The modeling results suggest that at concentration levels up to 70% Ar the dominant growth species is $CH_3$, and this changes to $C_2H$ above 70 vol.% Ar. There is also an accompanying change in the morphology of

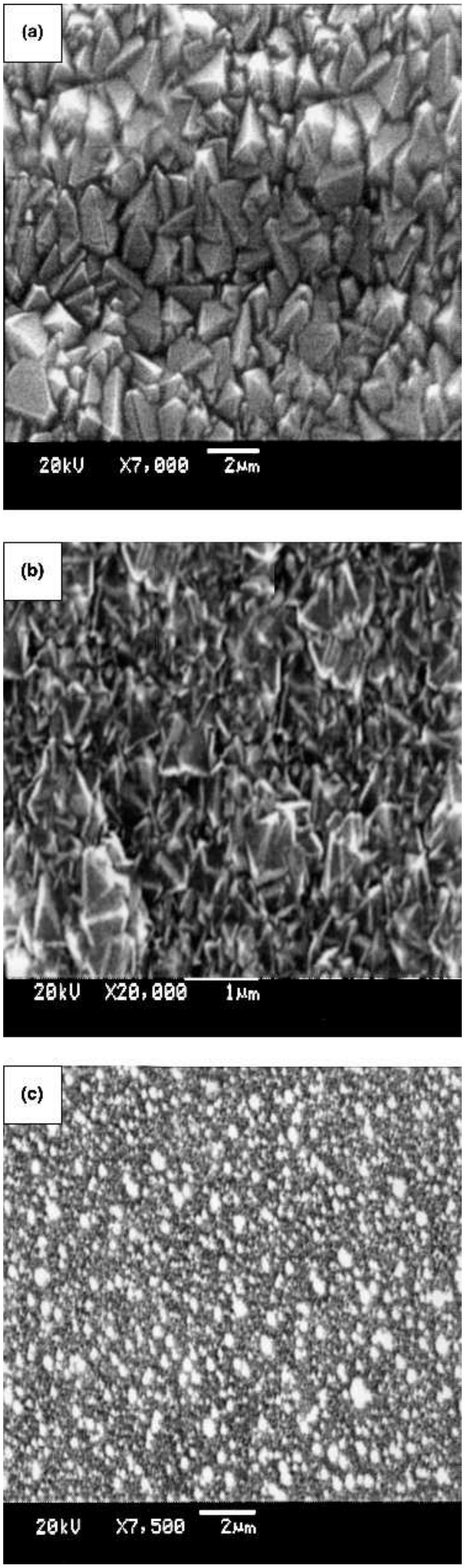

**Fig. 1** SEM images of diamond films grown on titanium alloy for 4 h in (a) 0, (b) 90, and (c) 98 vol.% Ar

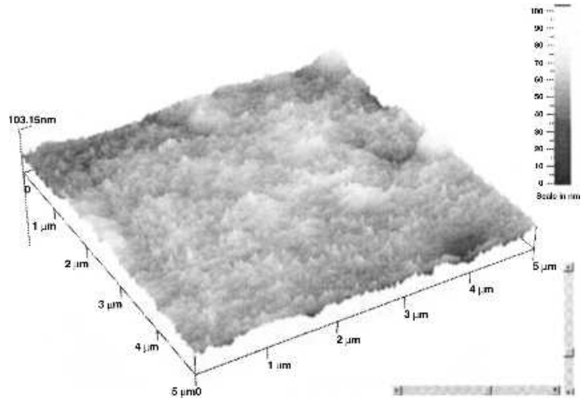

**Fig. 2** AFM image of diamond films grown on Ti-6Al-4V. The surface roughness = 54.14 nm. 5 by 5 μm scanned area in the tapping mode

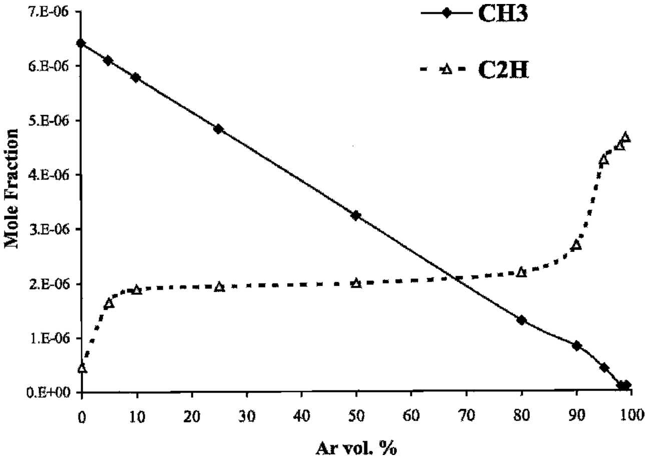

**Fig. 3** Graph of $CH_3$ and $C_2H$ mole fractions plotted against a function of Ar vol % at 2200 K and 2660 Pa

the film as described earlier. Modeling results of mole fraction as a function temperature for all of the gas species at 2660 Pa using 99% Ar and 1% $CH_4$ is shown Fig. 4. There is a rapid decrease in the precursor species $CH_4$ and $C_2H_4$ with temperature. Hydrogen and $C_2H$ show a steep increase with temperature, and as noted previously the acetylene concentration remains reasonably constant regardless of temperature.

## 4. Conclusions

In this study, we have demonstrated that nanocrystalline films may be deposited using Ar dilution to the $CH_4/H_2$ mixtures. At higher concentrations of Ar additions, the diamond film structure, uniformity, and morphology alter significantly. A variation from microcrystalline to NCD films is observed. The modeling results show that the gas phase chemistry is altered from $C_1$ growth species to $C_2$ using Ar concentrations >70 vol.%. At these concentrations, the $C_2$ dimer dominates the gas phase chemistry. Modeling the effects of Ar to the gas phase chemistry is a valuable instrument to control crystallinity, structure, and the surface properties of the diamond film.

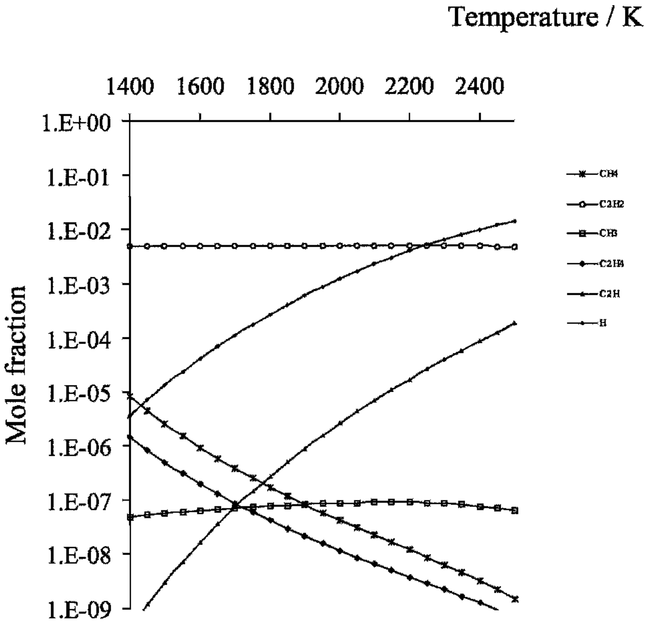

**Fig. 4** Mole fractions of the gas species plotted as a function of temperature using 99% Ar/1% $CH_4$ at 2660 Pa

## References

1. J.C. Angus and C.C. Hayman, Low Pressure, Metastable Growth of Diamond and Diamond-Like Phases, *Science,* Vol 241, 1988, p 913-920
2. R. Erz, W. Dotter, K. Jung, and H. Ehrhardt, Preparation of Smooth and Nanocrystalline Diamond Films, *Diamond Relat. Mater.,* Vol 2, 1993, p 449-453
3. L.C. Qin, D. Zhou, A.R. Krauss, and D.M. Gruen, TEM Characterization of Nanodiamond Thin Films, *Nanostruct. Mater.,*Vol 10, 1998, p 649-660
4. H.-G. Busmann, U. Brauneck, and H.-W. David, Fullerenes as the Parent Molecule for the Deposition of Tetrahedral Carbon, *Carbon,* Vol 36, 1998, p 529-533
5. A. Erdemir, G. Fenske, A. Krauss, D.T. Gruen, T. McCauley, and R. Csensits, Tribological Properties of Nanocrystalline Diamond Films, *Surf. Coat. Technol.,* Vol 120-121, 1999, p 565-572
6. J.M. Lopez, F.J. Gordillo-Vazquez, and J.M. Albella, Nanocrystalline Diamond Thin Films Deposited by 35 kHz Ar-Rich Plasmas, *Appl. Surf. Sci.,* Vol 185, 2002, p 321-325
7. P. Keblinski, S.R. Phillpot, D. Wolf, and H. Gleiter, On the Nature of Grain Boundaries in Nanocrystalline Diamond, *Nanostruct. Mater.,* Vol 12, 1999, p 339-344
8. T. Lin, A. Wee, Z. Shen, J. Lin, C. Lai, Q. Gao, and T. Zhang, High-Resolution Transmission Electron Microscopy Study of the Initial Growth of Diamond on Silicon, *Diamond Relat. Mater.,* Vol 9, 2000, p 1703-1707
9. M. Hiramatsu, K. Kato, C.H. Lau, J.S. Foord, and M. Hori, Measurement of C2 Radical Density in Microwave Methane/Hydrogen Plasma Used for Nanocrystalline Diamond Film Formation, *Diamond Relat. Mater.,* Vol 12, 2003, p 365-368
10. J.E. Butler, Optical Probing of Diamond Chemical Vapor Deposition, *Carbon,* Vol 28, 1990, p 809
11. C. Zuiker, R. Krauss, D. Gruen, X. Pan, J.-C. Li, R. Csensits, A. Erdemir, C. Bindel, and G. Fenske, Physical and Tribological Properties of Diamond Films Grown in Argon Carbon Plasmas, *Thin Solid Films,* Vol 270, 1995, p 154-159
12. P.K. Bachmann and W. van Enckevort, Diamond Deposition Technologies, *Diamond Relat. Mater.,* Vol 1, 1992, p 1021-1034
13. P. John, J.R. Rabeau, and J.I.B. Wilson, The Cavity Ring-Down Spectroscopy of C2 in a Microwave Plasma, *Diamond Relat. Mater.,* Vol 11, 2002, p 608-611
14. W. Ahmed, C. Rego, A. Afzal, N. Ali, and I. Hassan, CVD Diamond: Controlling Structure and Morphology, *Vacuum,* Vol 56, 2000, p 153-158
15. I.U. Hassan, C.A. Rego, N. Ali, W. Ahmed, and I.P. O'Hare, An Investigation of the Structural Properties of Diamond Films Deposited by Pulsed Bias Enhanced Hot Filament CVD, *Thin Solid Films,* Vol 355-356, 1999, p 134-138
16. A.N. Jones, W. Ahmed, I.U. Hassan, C.A. Rego, and H. Sein, Pulsed Biased Growth of Nanocrystalline Diamond by HFCVD, *Surf. Eng.,* Vol 20, 2004, p 181-185
17. R. J. Lee and F.M. Rupley, Gas Phase Composition during Chlorine-Assisted CVD of Diamond: A Molecular Beam Study, *J. Appl. Phys.,* Vol 79, 1995, p 7264-7273
18. M. Frenklach, H. Wang, and M. Rabinowitz, Optimization of Large Chemical Kinetic Mechanisms Using Solution Mapping Method, *J. Prog. Energy Combust. Sci.,* Vol 18, 1992, p 47-56
19. J. W. C. G. Warnatz, Ed., *Combustion Chemistry,* Springer-Verlag, New York, 1984
20. A.F. Wagner and D.M. Wardlaw, Combustion in Chemical Systems, *J. Phys. Chem.,* Vol 92, 1988, p 2462-2465
21. P.H. Stewart, G.P. Smith, and D.M. Golden, Pressure and Temperature Dependence of Methane Decomposition, *Int. J. Chem. Kinet.,* Vol 21, 1989, p 923-924
22. T. Bohland, S. Dobe, F. Temps, and H.G. Wagner, Chemical Reactions in Gaseous Atmospheres, *Ber. Bunsenges. Phys. Chem.,* Vol 89, 1989, p 1110-1115
23. N.R. Cohen, Are Reaction Rate Coefficients Additive? *Int. J. Chem. Kinet.,* Vol 23, 1991, p 397-417
24. J.E. Butler, J.W. Fleming, L.P. Goss, and M.C. Lin, Reaction Rate Coefficients in Complex Systems, *Am. Chem. Soc. ACS Symp. Ser.,* 1980, p 397-403, series 134
25. J.A. Miller and C.T. Bowman, Mechanisms and Modeling of Nitrogen Chemistry in Combustion, *Prog. Energy Combust. Sci.,* Vol 15, 1989, p 287-294
26. A.J. Dean, D.F. Davidson, and R.K. Hanson, Modeling of Gas Species in Complex Gas Systems, *J. Phys. Chem.,* Vol 95, 1991, p 183-185
27. S. Zabarnick, J.W. Fleming, and M.C. Lin, Kinetic Studies of Reactions in Carbon-Based Systems, *J. Chem. Phys.,* Vol 85, 1986, p 4375-4376
28. S. Bauerle, M. Klatt, and H.G. Wagner, Kinetic Studies in Gases Involving Hydrogen and Methane, *Ber. Bunsenges. Phys. Chem.,* Vol 99, 1995, p 870-881